OXIDATIVE DEHYDROGENATION OF ETHANE ON VANADIUM-CONTAINING ALUMINOPHOSPHATES WITH AFI STRUCTURE

Teresa BLASCO[a1], Patricia CONCEPCION[a], Jose M. LOPEZ NIETO[a2,*] and Arturo MARTINEZ-ARIAS[b]

[a] *Instituto de Tecnologia Quimica, Universidad Politecnica, UPV-CSIC, 46022-Valencia, Spain; e-mail: [1] tblasco@itq.upv.es, [2] jmlopez@itq.upv.es*

[b] *Instituto de Catalisis y Petroleoquimica, Campus UAM-Cantoblanco, 28049-Madrid, Spain; e-mail: amartinez@icp.csic.es*

Received June 25, 1998
Accepted September 8, 1998

MeAPO-5 (Me = V, Mg, Co, Mn) and VMeAPO-5 (Me = Mg, Co, Mn) with AFI structure were prepared by hydrothermal synthesis and characterized by nitrogen-adsorption, TPR, diffuse reflectance (UV-VIS) and ESR spectroscopies. Their catalytic performance in the oxidative dehydrogenation of ethane using molecular oxygen was also studied. Although different catalytic behaviour was observed depending on the metal incorporated, Vanadia-metal containing materials were the most selective catalysts. The importance of both redox and acid character of the catalysts on their catalytic properties is discussed.

Key words: Aluminophosphate; Microporous materials (VAPO-5, VMeAPO-5); Vanadium based catalysts; Oxidative dehydrogenation of propane; Heterogeneous catalysis; Zeolites.

During several decades zeolites have found many applications as catalysts in the oil refining and petrochemical industry[1–3]. The characteristics of zeolites and zeotypes, *i.e.* a regular three-dimensional crystal structure with pores of molecular dimensions, shape-selectivity control of reaction selectivity, as well as their possible modifications by isomorphous substitution (incorporating and/or modifying acid and redox properties), are of great interest for designing effective catalysts for oxidation of alkanes, as well as for a variety of selective oxidation reactions in liquid phase[1–3].

The introduction of transition metal cations into ZSM-5 (refs[4–6]) or silicalite[7–10] strongly enhances the catalytic activity and selectivity for oxidative dehydrogenation (ODH) of ethane or propane, respectively, and indeed, V-silicalite appears to be one of the most selective catalysts in the ODH of propane to propene using either O_2 or N_2O as oxidant[7–9]. Although aromatic hydrocarbons are obtained on these catalysts with

* The author to whom correspondence should be addressed.

selectivities which depend on the reaction conditions, oxygen-containing products other than carbon oxides are not observed in any case.

In addition to zeolites, also microporous aluminophosphates with the AFI structure have been studied as catalysts in the oxidation of short-chain paraffins. Pure $AlPO_4$-5 shows a low activity in the ODH of propane[11,12] and ethane[13–16] but its catalytic performance is strongly enhanced by the incorporation of metals by isomorphous substitution, *i.e.* VAPO-5 (refs[11,12,17]), CoAPO-5 (ref.[15]) and MnAPO-5 (ref.[18]), being those the most promising catalysts[11,13].

An important aspect of V-containing microporous materials, in particular V-silicalite and VAPO-5, is related to the products distribution achieved in oxidation reactions as they are selective catalysts in the ODH reactions but show a low selectivity in N- or O-insertion in the ammoxidation and oxidation of alkylaromatics[19–22] and alkanes[23]. Moreover, it has been shown that the simultaneous incorporation of both Mg^{2+} and V^{5+} ions in aluminophosphates with the AFI structure gives rise to VMgAPO-5 catalysts selective in the oxidation of ethane to ethene[13,24]. Since it is known that in Me(II)APO-5, Me^{2+} (Me = Mg, Co, Mn) substitutes for Al^{3+} to create acid sites[25,26], both redox and acid centres are expected to be present in VMe(II)APO-5 materials[24,27].

The aim of this paper is to study the effect of the incorporated divalent cations on the catalytic behaviour of Me(II)APO-5 and VMe(II)APO-5, for Me = Mg, Co and Mn in the oxidative dehydrogenation of ethane using molecular oxygen as oxidant. From the results presented here, it will be concluded that the nature of the bivalent metal cation determines both the degree of isomorphous substitution and the catalytic properties of metal-containing $AlPO_4$-5.

EXPERIMENTAL

Synthesis

MeAPO-5 and VMeAPO-5 materials with different metal contents were obtained by hydrothermal synthesis, using triethylamine (TEA) as template, from gels with a $Al_2O_3/P_2O_5/V_2O_5/MeO/H_2O/Et_3N$ molar ratio of $0.8 : 1 : x : y : 47 : z$, with x, y and z values as indicated in Table I. Vanadium was incorporated as a V_2O_5/Et_3N solution, and the other metals, Mg, Co or Mn, were added in aqueous solution of corresponding salts. Orthophosphoric acid (Riedel, 85 wt.%), pseudo-bohemite (Catapal B Vista, 70 wt.% Al_2O_3), triethylamine (Aldrich, 99 wt.%) were also employed.

The synthesis procedure was described in ref.[24]. The gels were introduced in 60 ml Teflon-lined stainless steel autoclaves and heated in static conditions at 473 K for 16 h. The samples were centrifuged at 10 000 r.p.m, washed with deionized water and dried at 373 K overnight. Chemical composition of both the starting gels and the calcined solid products, as well as their crystallinities are given in Table I. Portions of the samples were calcined in dry air at 873 K for 8 h. The catalysts will be assigned as MeAP and VMeAP, with Me = Co, Mg or Mn.

Characterization

Chemical analyses of Mg, V, Co or Mn were done by atomic absorption spectroscopy and P was determined by a colorimetric method using the complex formed between phosphorus and molybdovanadic acid[28]. The BET surface area of the samples, S_{BET}, was obtained in an ASAP 2000 apparatus, following the BET method from N_2 adsorption isotherms at 77 K and taken a value of 0.164 nm^2 for the cross-section of N_2.

X-Ray diffraction (XRD) was performed on a Phillips 1060 diffractometer provided with graphite monochromator employing nickel-filtered CuKα radiation. Crystallinity was determined by measuring the intensity of the peaks appearing at 2θ = 19.8, 21.1 and 22.4 degree and comparing them with that of uncalcined $AlPO_4$-5.

Diffuse reflectance (DR) spectra in the UV-VIS region were collected with a Shimadzu UV-2010 PC spectrophotometer equipped with a reflectance attachment. Different references, V_2O_5, NH_4VO_3, vanadyl oxalate, were used[12].

Electron spin resonance (ESR) spectra were recorded at 77 K on a Bruker ER 200D-SRC spectrometer working at the X-band. The *g* values of the paramagnetic species in the samples were measured using DPPH (*g* = 2.0036) as an standard. Quantitative analysis was carried out by double integration, using $CuSO_4$ for calibration. Before recording the spectra, the calcined catalyst were re-oxidized at 773 K with 40 000 Pa of oxygen for 1 h. The reduced samples were prepared by heating the calcined materials (previously evacuated at 298 K) with 13 300 Pa of H_2 at temperatures in the range 373–773 K for 1 h. All samples, re-oxidized or reduced, were degassed at room temperature until a final pressure of 10^{-5} Pa prior to the spectra acquisition.

Temperature programmed reduction (TPR) results were obtained in a Micromeritics apparatus. Samples of 100 mg were first treated in argon at room temperature for 1 h, and subsequently contacted with H_2/Ar mixture (molar ratio of 0.15, total flow of 3 l h^{-1}) and heated, at a rate of 10 K min^{-1}, to a final temperature of 1 273 K.

TABLE I
Composition and characteristics of MeAPO-5 and VMeAPO-5 catalysts

Catalyst	Molar ratio in gel			gel pH	Metal loading[a] wt.%		Yield[b] %	Crystallinity[c] %
	Et_3N	V_2O_5	MeO_x		V	Me		
VAPO (1)	1.76	0.12	0	5.6	0.57	0	11.7	100
VAPO (2)	1.76	0.24	0	4.6	1.15	0	[d]	70
MgAPO (1)	1.50	0	0.02	6.5	0	0.16	14.0	100
MgAPO (2)	1.50	0	0.10	4.9	0	1.00	18.1	53
VMgAPO	1.50	0.12	0.20	4.5	0.53	2.68	18.3	71
CoAPO	1.50	0	0.02	5.7	0	0.79	13.0	99
VCoAPO	1.50	0.06	0.02	5.4	0.37	0.88	11.3	86
MnAPO	1.50	0	0.05	5.3	0	0.47	13.0	98
VMnAPO	1.50	0.24	0.05	4.9	0.64	0.49	10.4	90

[a] Metal content in calcined samples. [b] Yield (solid/gel in g/g). [c] Crystallinities of AFl structure of calcined samples are referred to pure $AlPO_4$-5. [d] Not determined.

Catalytic Test

Catalytic tests for the oxidative dehydrogenation of ethane were carried out in a fixed-bed quartz tubular reactor (16 mm i.d., 500 mm length) equipped with a coaxial thermocouple for measuring the temperature profiles. Catalyst samples from 0.5 to 2.0 g (particle size between 0.42 and 0.59 nm) were mixed with variable amounts of SiC to keep a constant volume in the catalyst bed of 3 cm^3. The reaction was studied at 793–873 K using an ethane/oxygen/helium molar ratio of 4 : 8 : 88. The total flow was varied from 6 to 12 l h^{-1} to obtain different contact times (*W/F*). Analysis of reactants and products was carried out using gas chromatography, and two different columns, Porapak Q (3.0 m × 1/8 in.) and molecular sieve 5A (1.5 × 1/8 in.). Blank runs at 723–873 K were carried out with pure SiC, at the lowest total flow used in this study (6 l h^{-1}). Under our reaction conditions the presence of homogeneous reaction can be neglected.

RESULTS AND DISCUSSION

Catalyst Characterization

Table I summarizes chemical composition of the synthesis gel as well as the main characteristic of the final materials. As can be seen there, all VMeAP samples contain about 0.6–0.7 wt.% of vanadium, except sample VCoAP with only a 0.37 wt.% of V. Comparison of the Me(II) content in MeAPO-5 and VMeAPO-5 (Table I) indicates that the presence of V in the synthesis gel causes an increase in the Mg^{2+} concentration (sample VMgAP), whereas it has no effects on the final amount of Me(II) in VCoAP or VMnAP catalysts. On the other hand, the content of divalent cations in MeVAP samples increases as follows: $Mn^{2+} < Co^{2+} < Mg^{2+}$, while the ionic radii of Mn^{2+}, Co^{2+} and Mg^{2+} (0.805, 0.72 and 0.707 Å, respectively[26]) decrease in the opposite order, which suggests that the incorporation of divalent metals is favoured for smaller cations. This hypothesis is further supported by recent ^{31}P MAS NMR results which indicate an effective incorporation of Mg^{2+} to the framework positions in VMgAP (ref.[27]).

The XRD patterns of the V, Me and VMe-containing aluminophosphate studied here, both as synthesized and calcined, are characteristic of highly crystalline AFI structure ($AlPO_4$-5) (Table I), and amorphous aluminophosphates was only observed when sample MnAP was calcined above 873 K. No crystallinity loss was detected after the catalytic test, except for sample VMnAP when the reaction was carried out at 873 K.

In order to determine the state of reducible cations, DR (UV-VIS) and ESR spectroscopy have been employed, while the catalyst reducibility has been followed by TPR. Table I summarizes the temperature maxima of hydrogen consumption (T_m) during the TPR experiments. All samples show an additional broad peak at about 900–973 K associated with the formation of reduced compounds during the degradation MeAPO-5 materials[12,28].

A) VAPO-5 and VMgAPO-5. The UV-VIS DR spectra of VAP and VMgAP samples (Fig. 1a), present a band at 270–280 nm assigned to isolated tetrahedral V^{5+}, as already discussed in previous papers[12,24]. The fact that most of the vanadium present must be as

V^{5+} is confirmed by ESR, since the spectral intensity accounts for only 3% of the total vanadium.

The ESR spectrum of calcined VAP sample (Fig. 2a) consists of an hyperfine structured axially symmetric signal V1, with $g_{||} = 1.927$, $g_{\perp} = 1.980$, $A_{||} = 17.5 \cdot 10^{-3}$ cm^{-1}, $A_{\perp} = 7.2 \cdot 10^{-3}$ cm^{-1}, characteristic of isolated VO^{2+} ions in distorted octahedral or square pyramidal environments[12,29–31]. Upon reducing the sample in H_2, the concentration of paramagnetic vanadium increases up to 8% at $T_r = 673$ K, while a certain decrease in the overall intensity is produced at $T_r = 773$ K. As shown in Fig. 3b, at that temperature the spectrum is mainly formed by the overlapping signals V2 ($g_{||} = 1.917$, $g_{\perp} = 1.981$, $A_{||} = 18.8 \cdot 10^{-3}$ cm^{-1}, $A_{\perp} = 7.5 \cdot 10^{-3}$ cm^{-1}) and V3 ($\langle g \rangle = 1.972$). Signal V2 is similar to that obtained in V^{4+}-doped α-cristobalite $AlPO_4$ and is attributed to V^{4+} ions in a relatively strongly distorted tetrahedral symmetry, which suggests that the

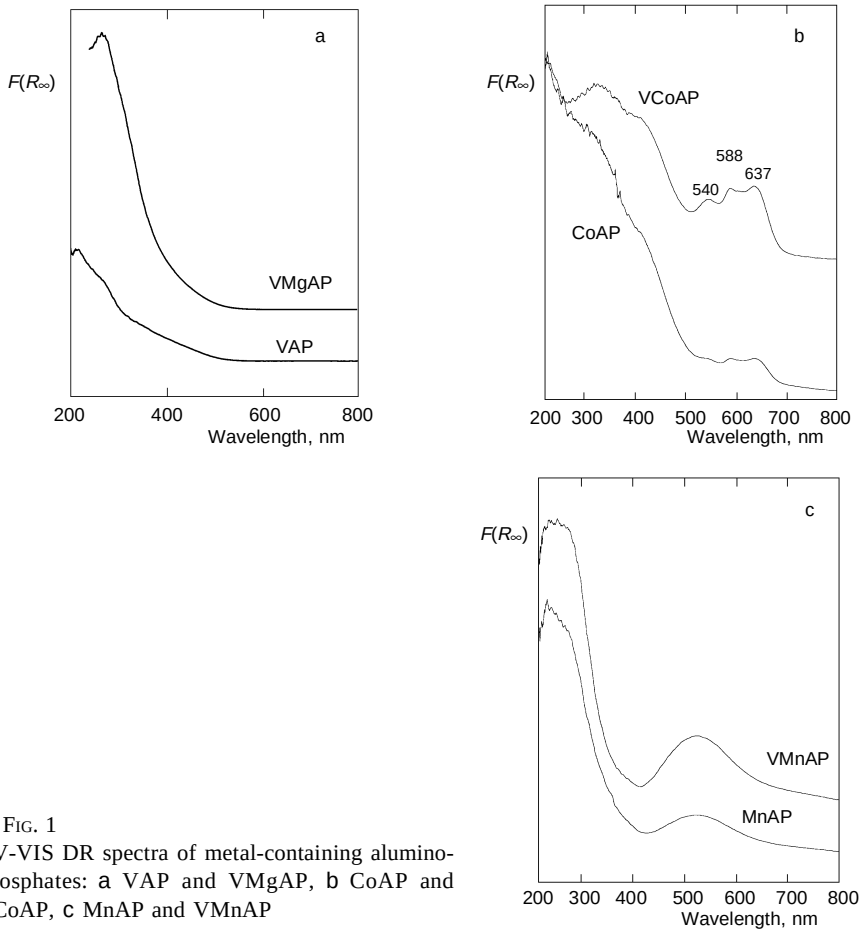

FIG. 1
UV-VIS DR spectra of metal-containing aluminophosphates: a VAP and VMgAP, b CoAP and VCoAP, c MnAP and VMnAP

corresponding V^{4+} ions could substitute framework Al^{3+} cations[29]. Signal V3 is assigned to associated V^{4+} species, whose origin must probably be the reduction of a pre-existing non-framework V_2O_5 oxidic phase.

Similar paramagnetic vanadium species have been observed in sample VMgAP, with an intensity that corresponds to 8% of the total V concentration in the calcined material. A comparison of the ESR spectra of samples VAP and VMgAP reduced at increasing temperatures show a significantly higher concentration of paramagnetic vanadium in the Mg baring material, yielding mainly isolated vanadyl species. For both samples, the decrease in the spin density observed when the reduction temperature is raised must be due to the formation of reduced diamagnetic vanadium species, which makes difficult to evaluate the reducibility of vanadium in V-containing aluminophosphates.

The TPR peak of reduction of V^{5+} to V^{4+} appears at 728 and 793 K in VAP and VMgAP samples (Table II), respectively, in agreement with previous results[12,24]. Then, the higher relative concentration of paramagnetic vanadium detected by ESR in the magnesium-containing aluminophosphate can tentatively be attributed to a stabilization effect of V^{4+} against reduction.

B) CoAPO-5 and VCoAPO-5. The DR spectra of Co-containing aluminophosphates calcined in air, CoAP and VCoAP (Fig. 1b), show broad bands at 310 and 400 nm which have been assigned to Co^{3+} species[32,33] or Co^{2+} species incorporated into the $AlPO_4$-5 framework in a distorted environment[34]. Also, three bands at 546, 588 and 636 nm,

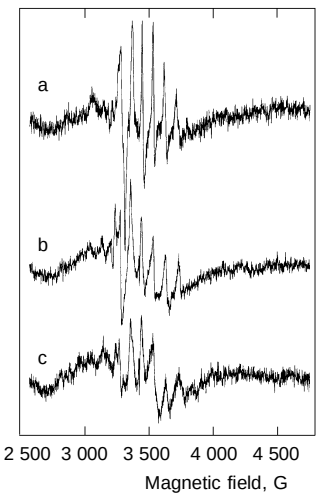

FIG. 2
ESR spectra of catalysts VAP (a and b) and VCoAP (c) after re-oxidation (a) and reduction at 773 K (b and c)

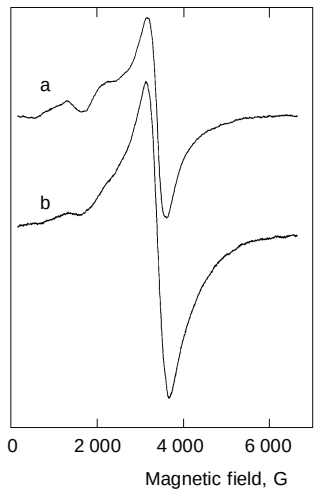

FIG. 3
ESR spectra of catalyst VMnAP re-oxidized (a) and reduced at 773 K (b)

attributed to the *d–d* transitions of Co^{2+} species in a tetrahedral coordination[35] can be observed, although weaker than in the as-synthesized form.

The presence of residual paramagnetic Co^{2+} cations in calcined VCoAP and CoAP materials is also confirmed by ESR. Both spectra (not shown) are similar and present very weak and broad absorption bands at $g \approx 4.7$ and in the range $g \approx 4.0$–1.8 typical of Co^{2+} species[33,34,36]. The weak and poor resolution of the paramagnetic spectra might be due to the diamagnetic nature of the cobalt species, *i.e.* they would behave as Co^{3+}, suggesting that the DR signals will mainly be due to trivalent cobalt. However, no definitive conclusion should be taken on the basis of ESR spectra as we cannot discard the presence of invisible Co^{2+} because of its short relaxation time. In CoAP catalyst the intensity of this signal increases after reduction with H_2, reaching a maximum at *ca* 573 K, whereas for VCoAP, the signal of paramagnetic Co^{2+} vanishes above 473 K, appearing at the same time very weak signals of vanadyl species (probably of type V2 and V3) (Fig. 2c).

The TPR pattern of calcined CoAP sample (Table II) presents a broad and weak peak at 928 K previously observed in MeAPO-5 materials attributed to the formation of reducible compounds during the thermal decomposition of the molecular sieve[28]. However, when the as-synthesized sample was calcined *in situ*, *i.e.*, with dry oxygen, before the TPR experiments, a new peak at 703 K appeared. The origin of this peak may be the reduction of Co^{3+}, formed during the calcination step, to Co^{2+} when carried out in the absence of water. Since the ESR spectra were recorded after calcination in the absence of water, the low intensity of paramagnetic Co signals can be explained, at least, in part, by the main presence of Co^{3+}.

TABLE II
Reducibility (T_m) and nature of Me- and V-species in VMeAPO-5

Catalyst	T_m[a], K	Me- and V-species[b]					Reference
		as-synthesized		calcined			
VAPO (1)	728	V^{4+}		V^{5+}			17
MgAPO	–		Mg^{2+}		Mg^{2+}		29
VMgAPO	793	V^{4+}	Mg^{2+}	V^{5+}	Mg^{2+}		18, 28
CoAPO	928 (706)[c]		Co^{2+}		Co^{2+}	Co^{3+}	this paper
VCoAPO	628, 733	V^{4+}	Co^{2+}	V^{5+}	Co^{2+}	Co^{3+}	this paper
MnAPO	573, 898		Mn^{2+}		Mn^{2+}		this paper
VMnAPO	573, 788, 933	V^{4+}	Mn^{2+}	V^{5+}	Mn^{2+}	Mn^{3+}	this paper

[a] Temperature maxima of the hydrogen consumption (T_m). [b] Determined by DR UV-VIS. [c] TPR results on previously calcined samples.

The TPR pattern of VCoAP shows, in addition to a broad peak at high temperature, two reduction peaks at 628 and 733 K. The latter also appeared in VAPO-5 (ref.[12]) and then it is probably due to the reduction of V^{5+}, while the peak at 628 K is ascribed to the reduction of Co^{3+}. However, it appears that the hydrogen-consumption associated with the last peak is lower than that calculated theoretically, suggesting that the concentration of reducible Co^{3+} species in VCoAP sample is low.

C) MnAPO-5 and VMnAPO-5. The DR spectra of as-synthesized MnAP and VMnAP samples (white in colour) show a band at 268 nm that can be attributed to octahedral Mn^{2+} cations[37]. After calcination (Fig. 2c), samples turn pink and give a broad band at 523 nm which has been related to changes in the electronic environment of Mn^{2+} species[37] although they can be oxidized to Mn^{3+} species during calcination at temperatures higher than 475 K (the materials behaves reversibly in redox cycles at temperatures near 500 K) (ref.[38]).

The presence of paramagnetic divalent manganese cations in MnAP (not shown) and VMnAP (Fig. 3a) has also been observed by ESR. The spectra of both calcined samples consist of a broad symmetric signal centred at $g \approx 2.0$ (signal M1) superimposed to broad and weak peaks at $g \approx 5.5$ and $g \approx 3.2$ (signal M2) (see Fig. 2a). Signal M1 must be due to Mn^{2+} ions interacting with each other[39,40], whereas signal M2 is assigned to Mn^{2+} in environments experiencing orthorhombic distorsions[41,42]. The main difference between MnAP and VMnAP is the lower intensity of species M2 in the vanadium-free catalyst, although both samples behave in a similar way against reduction. Figure 3b depicts the ESR spectrum of sample VMnAP heated with H_2 at 773 K that shows a decrease in the linewidth of signal M1, which can be attributed to an increase in the exchange interaction between Mn^{2+} cations due to a decrease in the average distances between each other. This effect is more pronounced in the V-containing aluminophosphate.

The TPR pattern of sample MnAP (Table II) is characterized by the presence of two peaks at 573 and 898 K which can be related to the reduction of Mn^{3+} and Mn^{2+}, respectively. In the case of the VMnAP sample (Table II), a new peak at 788 K could be due to the reduction of V^{5+} species as it was proposed for VAPO-5 (ref.[12]). The fact that no V^{4+} signals are detected by ESR in sample VMnAP after reduction with H_2 at elevated temperatures may indicate that V^{5+} has been reduced to an oxidation state lower than +IV.

From ESR and TPR experiments, it can be concluded that the redox behavior of vanadium atoms depends on the divalent cation incorporated into the framework. While some paramagnetic V^{4+} signal is always present in the ESR spectra of VAP (Figs 2a and 2b), in VCoAP it is only observed after reduction with H_2 above 373 K (Fig. 2c) and undetected in VMnAP even after reduction with H_2 up to 773 K (Fig. 3b). However, no definitive conclusions on the reducibility of vanadium can be obtained from ESR as both more oxidized and reduced states are ESR-silent.

Again, TPR experiments indicate that the reducibility of V^{5+} depends on the nature of Me(II) cations, in the VMgAP sample reduced at a higher temperature.

The IR study of adsorption–desorption of pyridine on VMeAPO-5 catalysts has been used to evaluate their acid properties. The IR spectra of representative samples evacuated at 523 K after adsorption of pyridine at 298 K are shown in Fig. 4. From this figure it is evident that V,Me-containing catalysts exhibit Brönsted (1 550 cm^{-1}) and Lewis (1 450 cm^{-1}) acid sites, as also observed for MeAPO-5 (Me = Mg, Co or Mn) (ref.[24]), while no pyridine is retained on VAPO-5 after degassing at 523 K (ref.[12]). Therefore, the observed acidity can be ascribed to the isomorphous substitution of Al^{3+} by Mg^{2+}, Co^{2+} or Mn^{2+}.

Catalytic Tests in the Oxidative Dehydrogenation of Ethane

The catalytic results obtained during the ODH of ethane on V-, Me- and VMeAPO-5 molecular sieves are shown in Table III. In all cases, ethene, CO and CO_2 were the only reaction products and no other oxygenated products were detected.

Figure 5 shows the dependence of the ethane conversion on the reaction temperature for the VMeAPO-5 catalysts. From these results, it can be concluded that the catalytic activity decreases in the order: VMnAP > VCoAP > MnAP > VAP > CoAP > VMgAP > MgAP, suggesting that the incorporation of reducible metal cations Me(II) (Co, Mn) into the VAPO-5 structure enhances the catalytic activity, whereas the introduction of Mg^{2+} has a negative effect. Comparison with the TPR results summarized in Table II shows a good correlation between catalyst reducibility and activity. Thus, the low catalytic activity of VMgAP catalyst could be explained by the low reducibility of vanadium.

Figure 6 presents the dependence of the selectivity to ethene on the ethane conversion at 853 K. The selectivity to ethene decrease as follows: VMgAP = VMnAP =

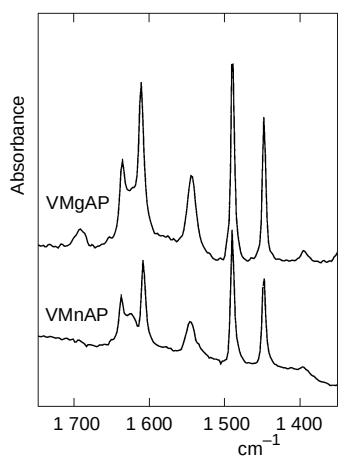

FIG. 4
FTIR spectra of adsorbed pyridine on VMnAP and VMgAP after outgassing at 623 K

VCoAP = MnAP > CoAP > VAP > MgAP. Thus, the best selectivities to ethene were observed on MnAP and VMe-containing catalysts.

Figure 7 displays the variation of the selectivities to the main reaction products, namely ethene, CO and CO_2, with ethane conversion at 853 K obtained during the oxidation of ethane on VCoAP catalyst. As it is evident from Fig. 7, when the ethane conversion increases, the selectivity to ethene decreases, CO increases, and the selectivity to CO_2 remains constant. Thus, it can be concluded that ethene is a primary and unstable product, CO is a secondary product, and CO_2 is a primary and stable product. This suggests the following reaction network.

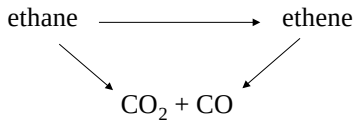

CO is preferentially formed by consecutive reactions from ethene and CO_2 is mainly formed by competitive reactions from ethane. Although kinetic constant values depend on the catalyst composition, the reaction scheme proposed above for VCoAP is also valid for all the other catalysts studied here.

TABLE III
Oxidative dehydrogenation of ethane on MeAPO-5 and VMeAPO-5 catalysts[a]

Catalyst	Temperature, K	Conversion, %	Selectivity, %		
			ethene	CO	CO_2
VAPO (1)	813	5.1	42.9	27.6	29.5
	853	12.4	43.6	36.6	19.8
MgAPO	873	4.1[b]	22.7	45.0	32.3
VMgAPO	793	2.0	71.2	12.4	17.5
	853	7.3	67.0	20.7	11.9
CoAPO	793	2.9	63.0	21.7	15.3
	853	10.3	55.5	34.7	9.8
VCoAPO	773	10.0	53.0	30.2	16.8
	813	19.3	55.7	30.0	14.3
MnAPO	773	7.6	69.8	16.0	14.0
	833	16.3	59.5	26.7	13.7
VMnAPO	773	9.7	61.4	28.8	9.8
	813	20.0	56.0	34.9	9.1

[a] Using 1 g of catalyst and a total flow of 200 ml (W/F = 50.9 g_{cat} h mol^{-1}_{ethane}). [b] W/F = 102 g_{cat} h mol^{-1}_{ethane} .

Figure 8 shows the productivities to ethene on all the catalyst. It can be seen that the best productivity to ethene is obtained on VCoAP and VMnAP catalysts, while very low values are observed for MgAP. The better catalytic performance of VMeAPO-5 materials could be due to a synergetic effect between two different phases, VAPO-5 and the corresponding MeAPO-5, intimately mixed. To check this, we present in Fig. 9 the productivity to ethene (in kg/kg h) obtained during the oxidation of ethane on pure MeVAPO-5 catalysts and the sum of those of VAP and the corresponding MeAPO-5. It comes out that while VCoAP and VMnAP give higher ethene productivities than the sum of the corresponding MeAPO-5 materials, similar values are obtained on VAP and VMgAP catalysts, although a better selectivity to ethene was obtained on VMgAP. These results support the effective incorporation of V and Co, Mn or Mg in the AFI structure.

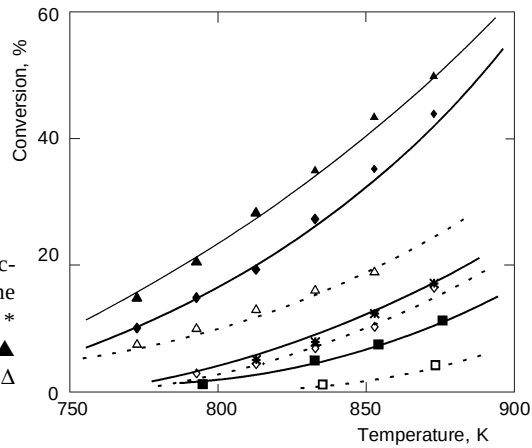

FIG. 5
Variation of the ethane conversion with reaction temperature in the oxidation of ethane on MeAPO-5 and VMeAPO-5 catalysts: * VAPO, ■ VMgAPO, ◆ VCoAPO, ▲ VMnAPO, ❒ MgAPO, ✧ CoAPO, Δ MnAPO (for reaction conditions, see text)

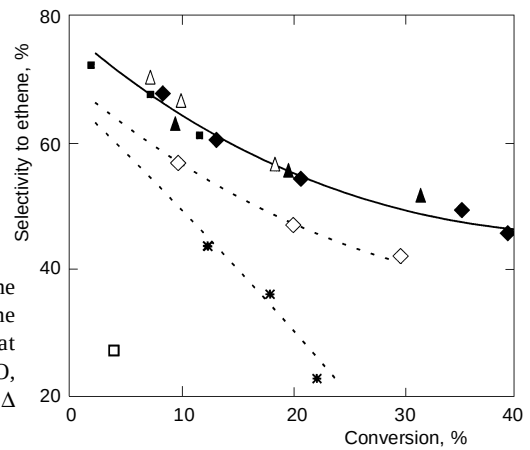

FIG. 6
Variation of the selectivity to ethene with the ethane conversion in the oxidation of ethane on MeAPO-5 and VMeAPO-5 catalysts at 853 K: * VAPO, ■ VMgAPO, ◆ VCoAPO, ▲ VMnAPO, ❒ MgAPO, ✧ CoAPO, Δ MnAPO

Recently, the selectivity to olefins during the ODH of alkanes on supported vanadium oxide catalysts[43,44] has been suggested to be influenced not only by the redox properties of the catalyst, but also by its acid-base character, in such a way that acid catalysts are more selective in the oxidative dehydrogenation of ethane to ethene than those with neutral or basic character[43–45]. According to this, VAPO-5, which does not display acid properties[18], gives the lowest selectivity to ethene, and MgAPO-5 catalysts possessing acid character (because of the substitution of Mg^{2+} by Al^{3+}), but without redox sites, shows a low activity in the ODH of ethane. VMgAPO-5 catalysts possess both Bronsted acid sites and redox sites (related to isolated V^{5+} ions) and then shows higher selectivity to ethene[24].

This interpretation can be generalized for the other VMeAPO-5 catalysts studied here. The higher selectivity to ethene on VMeAPO-5 catalysts than that of VAPO-5

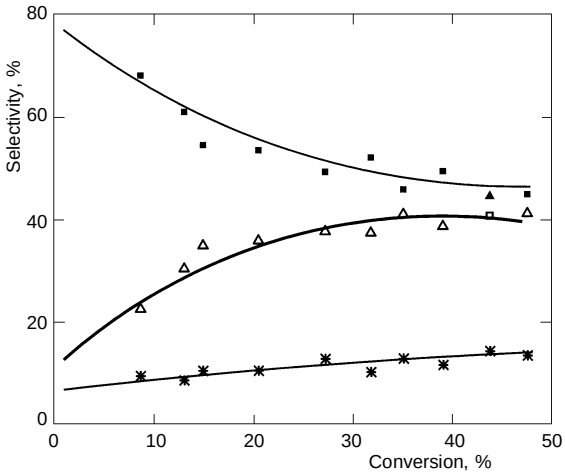

FIG. 7
Variation of the selectivity to the main reaction products, ■ ethene, Δ CO and * CO_2, with the ethane conversion in the oxidation of ethane on VCoAP catalyst (for experimental, see text)

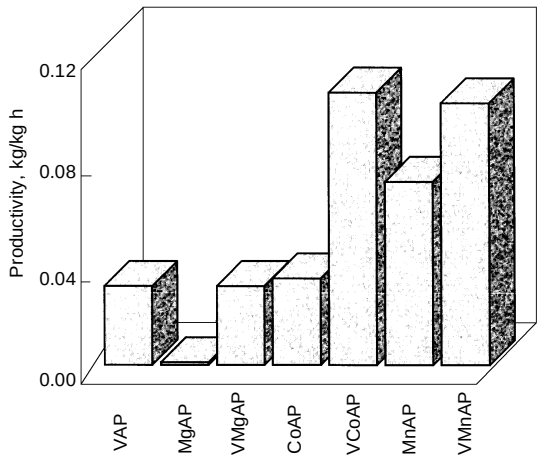

FIG. 8
Productivity to ethene on MeAPO-5 and VMeAPO-5 catalysts in the oxidation of ethane at 873 K

could be related to the presence of acid sites, originated by the isomorphous framework substitution of Al^{3+} by Me(II), *i.e.* Mg^{2+}, Co^{2+} or Mn^{2+}. Therefore, the catalytic behaviour of VMeAPO-5 in the ODH of ethane is a result of the presence of both acid and redox sites incorporated into the framework of the AFI structure.

On the other hand, the different catalytic activity of VMeAPO-5 catalysts could be due to differences in the incorporation and/or distribution of these metal cations in the aluminophosphate framework. In this sense, the presence of Me(II) cations in extra-framework positions would decrease the number of effective acid sites leading to lower activities. Although this possibility cannot be completely ruled out, the catalytic results presented here suggest that this is not probable.

An important factor in the catalytic activity of VMeAPO-5 materials to be considered is their redox properties. The different catalytic activity of Co- and Mn-containing materials with and without vanadium could tentatively be explained by differences in the oxidation state of the Me(II) cations. The results obtained here indicate the presence of Co^{3+} and Mn^{3+} in CoAPO and MnAPO when the calcination is carried out in a dry atmosphere, whereas also Co^{2+} and Mn^{2+} are present if water is present during calcination. Although mainly Co^{2+} and Mn^{2+} will be present under the reaction conditions, we cannot completely rule out the formation of oxidized species. Moreover, the addition of vanadium also modifies the catalyst reducibility. The TPR patterns of CoVAP and MnVAP samples show new H_2 consumption peaks probably related to the reduction of Co^{3+} to Co^{2+} and Mn^{3+} to Mn^{2+}, respectively as well as that of V^{5+} to V^{4+}. Therefore, cobalt and manganese in VMeAPO-5 materials could be partially stabilized as Co^{3+} and Mn^{3+} ions, producing a material similar to Me(III)Me(II)VAPO-5. A more detailed study of redox properties of these catalysts will be undertaken.

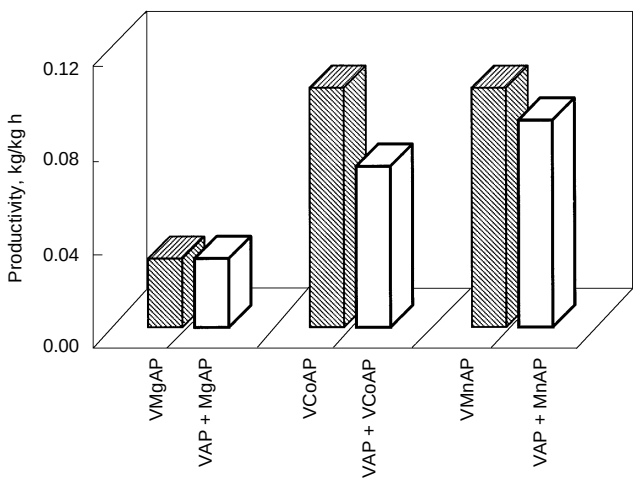

FIG. 9
Productivity to ethene on pure VMeAPO-5 and mixed VAPO-5 + MeAPO-5 catalysts

In conclusion, VMeAPO-5 catalysts are active and selective in the oxidative dehydrogenation of ethane. In our preparation conditions, both metals are incorporated into the framework of $AlPO_4$-5. The presence of both acid (related to Me(II) cations) and redox sites (probably related to V^{5+} or Me(III) cations) is an important factor to achieve a high selectivity during the ODH of ethane. However, in order to obtain an effective catalytic system, both sites must be at a short distance. The presence of extra-framework species in channels of microporous materials or the incorporation of a second reducible cation near to vanadium species could modify the catalytic activity of these materials.

Financial support from the Comisión Interministerial de Ciencia y Tecnologia in Spain (MAT 97-0561) is greatly appreciated.

REFERENCES

1. Venuto P. B.: *Microporous Mater.* **1994**, *2*, 297.
2. Corma A., Martinez A.: *Adv. Mater.* **1995**, *7*, 137.
3. Naber J. E., de Jong K. P., Stork W. H. J., Kuipers H. P. C. E., Post M. F. M.: *Stud. Surf. Sci. Catal.* **1994**, *84*, 2197.
4. Chang Y.-F., Somorjai G. A., Heinemann H.: *J. Catal.* **1995**, *154*, 24.
5. Chang Y.-F., Somorjai G. A., Heinemann H.: *Appl. Catal., A* **1993**, *96*, 305.
6. Kucherov A. V., Kucherova T. N., Slinkin A. A.: *Catal. Lett.* **1991**, *10*, 289.
7. Zatorski L. W., Centi G., Lopez Nieto J. M., Trifiro F., Bellusi G., Fattore V.: *Stud. Surf. Sci. Catal.* **1989**, *49*, 1243.
8. Centi G., Perathoner S., Trifiro F., Aboukais A., Aissi G. F.: *J. Phys. Chem.* **1992**, *96*, 2617.
9. Bellussi G., Centi G., Perathoner S., Trifiro F.: *ACS Symp. Ser.* **1993**, *523*, 281.
10. Centi G., Trifiro F.: *Appl. Catal., A* **1996**, *143*, 3.
11. Concepcion P., Lopez Nieto J. M., Perez-Pariente J.: *Catal. Lett.* **1993**, *19*, 333.
12. Blasco T., Concepcion P., Lopez Nieto J. M., Perez-Pariente J.: *J. Catal.* **1995**, *152*, 1.
13. Concepcion P., Lopez Nieto J. M., Perez-Pariente J.: *Catal. Lett.* **1994**, *28*, 9.
14. Concepcion P., Lopez Nieto J. M., Perez-Pariente J.: *Stud. Surf. Sci. Catal.* **1995**, *94*, 681.
15. Concepcion P., Corma A., Lopez Nieto J. M., Perez-Pariente J.: *Appl. Catal., A* **1996**, *143*, 17.
16. Wu J.-Y., Wan B.-Z.: *Ind. Eng. Chem. Res.* **1993**, *32*, 2987.
17. Concepcion P., Lopez Nieto J. M., Perez-Pariente J.: *J. Mol. Catal.* **1995**, *99*, 173.
18. Wan B.-Z., Huang K.: *Appl. Catal.* **1991**, *73*, 113.
19. Whittington B. I., Anderson J. R.: *J. Phys. Chem.* **1993**, *97*, 1032.
20. Centi G., Fazzini F., Canesson L., Tuel A.: *Stud. Surf. Sci. Catal.* **1997**, *110*, 893.
21. Ramachandra Rao R., Kulkarni S. J., Subrahmanyam M., Rama Rao A. V.: *Zeolites* **1996**, *16*, 254.
22. Kulkarni S. J., Ramachandra Rao R., Subrahmanyam M., Rama Rao A. V., Sarkany A., Guzci L.: *Appl. Catal., A* **1996**, *139*, 59.
23. Miyamoto A., Iwamoto Y., Matsuda H., Inui T.: *Stud. Surf. Sci. Catal.* **1989**, *49*, 1233.
24. Concepcion P., Lopez Nieto J. M., Mifsud A., Perez-Pariente J.: *Appl. Catal., A* **1996**, *151*, 373.
25. Concepcion P., Lopez Nieto J. M., Mifsud A., Perez-Pariente J.: *Zeolites* **1996**, *16*, 56.
26. Flanigen E. M., Lok B. M., Patton L., Wilson S. T.: *Stud. Surf. Sci. Catal.* **1986**, *28*, 103.

27. Blasco T., Concepcion P., Fernandez L., Lopez Nieto J. M., Martinez A: *Int. Congress on Zeolites, Baltimore, July 1998*, in press.
28. Roque-Malherbe R., Lopez-Cordero R., Gonzalez Morales J. A., Onate-Martinez J., Carreras-Gracial M.: *Zeolites* **1993**, *13*, 481.
29. Jhung S. H., Uh Y. S., Chon H.: *Appl. Catal.* **1990**, *62*, 61.
30. Weckhuysen B. M., Vannijvel I. P., Schoonheydt R. A.: *Zeolites* **1995**, *14*, 482.
31. Rigutto M. S., van Bekkum H.: *J. Mol. Catal.* **1993**, *81*, 77.
32. Montes C., Davis M. E., Murray B., Narayana M.: *J. Phys. Chem.* **1990**, *94*, 6425.
33. Iton L. E., Choi I., Desjasdins J. A., Maroni V. A.: *Zeolites* **1989**, *9*, 535.
34. Krushev V., Kevan L., Parrillo D. J., Pereira C., Kokotailo G. T., Gorte R. J.: *J. Phys. Chem.* **1994**, *98*, 10160.
35. Schoonheydt R. A., de Vos R., Pelgrims J., Leeman H.: *Stud. Surf. Sci. Catal.* **1989**, *49*, 559.
36. Chao K. J., Sheu S.-P., Sheu H.-S.: *J. Chem. Soc., Faraday Trans.* **1992**, *88*, 2949.
37. Parrillo D. J., Pereira C., Kokotailo G. T., Gorte R. J.: *J. Catal.* **1992**, *138*, 377.
38. Katzmarzyk A., Ernst S., Weitkamp J., Knozinger H.: *Catal. Lett.* **1991**, *9*, 85.
39. Goldfarb D.: *Zeolites* **1989**, *9*, 509.
40. Levi Z., Raitsimring A. M., Goldfarb D.: *J. Phys. Chem.* **1991**, *95*, 7830.
41. Schreurs J. W. H.: *J. Chem. Phys.* **1978**, *69*, 2151.
42. Rao A. S., Sreedhar B., Rao J. L., Lakshman S. V. J.: *J. Non-Cryst. Solids* **1992**, *144*, 169.
43. Blasco T., Lopez Nieto J. M.: *Appl. Catal., A* **1997**, *157*, 117.
44. Concepcion P., Galli A., Lopez Nieto J. M., Dejoz A., Vazquez M. I.: *Top. Catal.* **1996**, *3*, 451.
45. Blasco T., Galli A., Lopez Nieto J. M., Trifiro F.: *J. Catal.* **1997**, *169*, 203.